The effects of swing-leg retraction on running performance: analysis, simulation, and experiment

J. G. Daniël Karssen†, Matt Haberland‡*, Martijn Wisse† and Sangbae Kim‡

†*Department of BioMechanical Engineering, Delft University of Technology, Mekelweg 2, Delft, The Netherlands*
‡*Department of Mechanical Engineering, Massachusetts Institute of Technology, Cambridge, MA 02139, USA*

SUMMARY
Using simple running models, researchers have argued that swing-leg retraction can improve running robot performance. In this paper, we investigate whether this holds for a more realistic simulation model validated against a physical running robot. We find that swing-leg retraction can improve stability and disturbance rejection. Alternatively, swing-leg retraction can simultaneously reduce touchdown forces, slipping likelihood, and impact energy losses. Surprisingly, swing-leg retraction barely affected net energetic efficiency. The retraction rates at which these effects are the greatest are strongly model-dependent, suggesting that robot designers cannot always rely on simplified models to accurately predict such complex behaviors.

KEYWORDS: Legged robots; Bipeds; Robot dynamics; Human biomechanics; Biomimetic robots.

1. Introduction

Legged locomotion is an important topic in robotics because legged robots promise improved mobility in unstructured environments.[1–3] Intuition regarding the sensitivities of robot performance to hardware and controller parameters is essential for the design of effective legged mobility systems. In addition, knowledge of these sensitivities can give insight into human locomotion, which is useful for the design of better prostheses and orthoses. The goal of this paper is to develop intuition about the inherent effects of a particular control parameter, swing-leg retraction (SLR) rate, on several running performance metrics if possible, and otherwise identify trends that defy simple description.

Swing-leg retraction is a behavior exhibited by humans and animals in which the airborne front leg rotates rearward prior to touchdown.[4] It is hypothesized that swing-leg retraction enhances performance of biological systems,[5] and that we might use swing-leg retraction to improve the performance of legged robots, such as the Phides robot shown in Fig. 1. Use of swing-leg retraction to improve controller performance is attractive because it is a conceptually simple extension to any foot placement controller such as the constant angle of attack controller[6] and the neutral point controller.[7]

The effect of swing-leg retraction on limit cycle walking[8] is relatively well studied and has been shown to improve energy efficiency, small disturbance stability, and large disturbance rejection.[9–11] These results are illuminating for walking systems, but fundamental differences between walking and running gaits preclude the direct application of these results to running systems. Certain aspects of swing-leg retraction have been studied using relatively simple running models; for instance, multiple authors agree that swing-leg retraction can improve the stability of running;[5,6,12–15] conclude that low retraction rates yield better stability, but high retraction rates minimize peak forces;[14,16] and suggest that swing-leg retraction can improve energetic efficiency.[14,17,18] However, the existing literature leaves the following two important open questions:

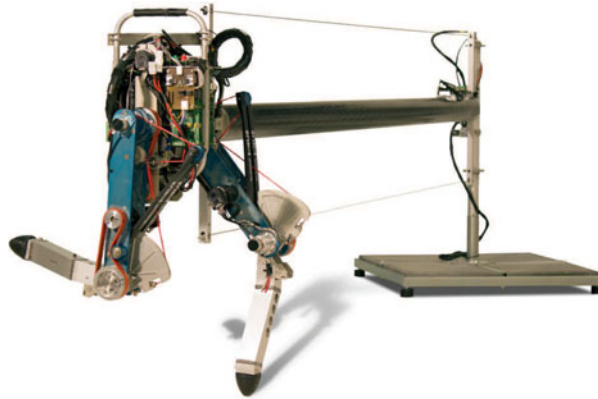
* Corresponding author. E-mail: mdhaber@mit.edu

Fig. 1. Running robot "Phides". This robot consists of a torso and two kneed legs with small, spherical feet. The robot is attached to a boom with a parallelogram mechanism to achieve planar behavior. The two hip joints are directly actuated by DC motors in the torso. The two knee joints are actuated by DC motors with a spring in series (torsion bar inside the knee shaft) as well as a spring in parallel (leaf spring with pulley mechanism).

- Do simple models accurately predict the effects of swing-leg retraction on a physical running robot?
- Given the effects of swing-leg retraction on different performance metrics, how should a controller's retraction rate be chosen?

The present paper provides answers to these questions through a study of the effects of swing-leg retraction on running performance using simple models, a realistic model, and physical hardware. The remainder of this paper is organized as follows: Section 2 introduces simulation models and experimental hardware used in this study. Sections 3 and 4 present the effects of the retraction rate on the impact losses and energetic efficiency of the models respectively. Section 5 discusses the effect of the retraction rate on the impact impulse and footing stability. Sections 6 and 7 study the effect of the retraction rate on the stability and disturbance rejection. The paper ends with a discussion, including model validation against physical robot, in Section 8, and conclusions in Section 9.

2. Models and Experimental Platform

In this study, our primary tool is simulation using a fairly complete rigid-body model (Fig. 4) of the running robot, Phides (Fig. 1). Physical experiments with Phides provide evidence that the realistic model is a representative of the actual machine. To better relate the findings to previous studies, we also compare the results of the realistic model simulations with those of simpler models. Whenever possible, the Spring Loaded Inverted Pendulum (SLIP, Fig. 2) model is used as a simple simulation model for comparison with refs. [5, 6, 12–15] . However, the SLIP model does not capture all the relevant dynamics; aspects related to energy loss and replacement are not captured because the model is energetically conservative, and other consequences of impact with the ground, such as reaction forces and foot slipping, cannot be studied accurately without leg mass. To study these, we use an extension of the SLIP, a Prismatic Leg model (Fig. 3) similar to that in ref. [14, 15, 18], and a new Kneed Leg model (Fig. 5), a simplification of the realistic model of Phides. Besides their utility as bridges to prior studies, these simple models permit either symbolic analysis or more efficient computation and help us gain insight by removing complexities of the realistic model.

To fairly compare the results of the simulation models and the robot, we match model parameters to the extent permitted by their structures. We normalize all parameters and results with the total mass M, leg length L_0, and gravitational acceleration g to get dimensionless numbers. For instance, the swing-leg retraction rate ω (in rad/s) is normalized as $\bar{\omega} = \omega \sqrt{\frac{L_0}{g}}$. Unless otherwise noted, the models and the robot run at normalized average speed $\dot{x}_{\mathrm{avg}}$ of 0.42 (Froude number of $0.18 = \dot{x}_{\mathrm{avg}}^2$). This is a slow speed for a running gait, but it is near the maximal speed of the physical robot.

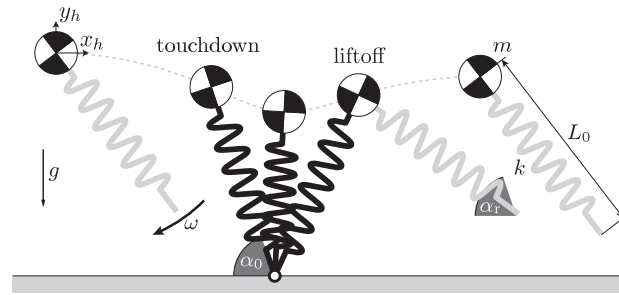The following sections give detailed descriptions of the simulation models and the physical robot.

Fig. 2. The SLIP model with swing-leg retraction. The model consists of a point mass body and a massless spring leg. At liftoff, the leg instantaneously assumes angle α_r with respect to the ground and begins rotating at rate ω. The leg angle at touchdown α_0 depends on the time between liftoff and touchdown.
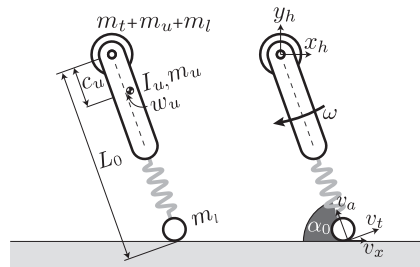

Fig. 3. Prismatic leg model, an extension of the SLIP model with distributed leg mass and a point mass foot.

2.1. SLIP model

2.1.1. Simulation. The SLIP model is a one-leg hopper model widely used for analyzing running dynamics.[6, 19–22] This model consists of a point mass body on a massless spring leg (Fig. 2). Despite its simplicity, it has been shown to be a reliable model for certain aspects of human and robot running, such as the center-of-mass trajectories.[23, 24]

Here the parameters of the SLIP model are chosen to match the robot Phides, with $m = 13.11$ kg, $L_0 = 0.58$ m, $g = 9.81$ m/s^2, and $k = 5.06$ kN/m, which are normalized as $\bar{m} = 1$, $\bar{L}_0 = 1$, $\bar{g} = 1$, and $\bar{k} = 22.8$.

2.1.2. Control of SLIP model. The SLIP model is controlled only by changing the angle of the spring leg during flight. Because the leg is massless, this requires no energy and does not affect the flight dynamics. However, this changes the angle α_0, the time, and thus the velocity, at which the leg touches the ground, which strongly influences the behavior during the stance phase.

In practice with the Phides robot, we found that the limited accuracy of sensors impedes reliable sensing of apex. So in this paper, we set the initial leg angle α_r and begin retraction at liftoff instead of at apex because liftoff can be measured with a simple contact switch. The start leg angle α_r is chosen to produce a limit cycle with a normalized apex horizontal speed of 0.42 and a normalized apex height of 1.04 regardless of the retraction rate.

2.1.3. Prismatic leg impact model. Because the SLIP model is energetically conservative, we use an extension of the SLIP model shown in Fig. 3 to study the effects of swing-leg retraction on the impact event. In the simple prismatic leg model, the mass of the SLIP is distributed to form the upper segment of the leg, and a point mass is added to the foot. The impact equations are derived according to conservation of angular momentum assuming a perfectly inelastic collision, that is, the foot sticks upon landing. Note that these equations are not used in the dynamic simulation of the SLIP model; these are only used in postprocessing to study the impact dynamics of a SLIP-like model with leg mass.

2.2. Realistic model

2.2.1. Simulation. The realistic simulation model is designed to closely resemble the physical running robot used in this study (Section 2.3). The model, shown in Fig. 4, is two-dimensional (planar) and consists of five rigid bodies: a torso, two upper legs, and two lower legs, the sizes and mass distributions
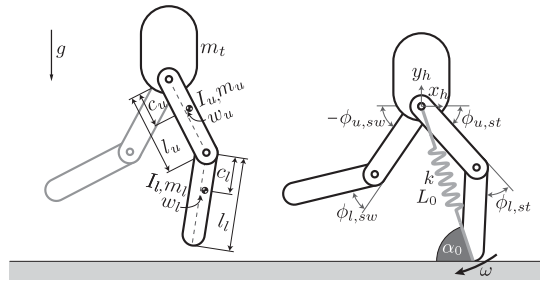
Fig. 4. Two-dimensional realistic running model that consists of five rigid bodies. The left figure shows the robot during the flight phase and labels model parameters, the values of which are given in Table I. The right figure shows the robot during the stance phase, during which the leg spring is active, and the six generalized coordinates are used to describe the motion. Note that the torso orientation is not a degree-of-freedom as the rotation of the torso is fixed with respect to the world.

of which are presented in Table I. The feet are simply points at the ends of the lower legs. For this study, we fix the rotation of the torso with respect to the world to eliminate the need to control the torso orientation. Torques, limited to 21.4 Nm to represent the actuator limitations of the robot, act at all four joints.

The running motion of the realistic model has two distinct phases: a flight phase, during which the robot is airborne, and a stance phase, in which one foot acts as a pin joint fixed to the ground. During the flight phase, the center of mass follows a ballistic trajectory, as the leg is not in contact with the ground, and the legs move under the influence of joint torques. When a foot touches the ground, the impact is modeled as an impulsive, perfectly inelastic collision. The state after impact is calculated according to angular momentum conservation. During stance, a spring of constant stiffness $k = 5.06$ kN/m (dimensionless stiffness of 22.8) produces a force linearly proportional to the difference between the leg length (distance from the stance foot to the hip) and its rest length $L_0 = 0.58$ m. The knee is equipped with an end stop, modeled as a unidirectional spring-damper, that prevents the leg from extending further than the rest length of the leg spring L_0. As in flight, joint torques control the robot during stance. Liftoff occurs and flight resumes when the normal force between the foot and the ground falls to zero. There is no impulsive collision involved, so there is no instantaneous change in state at liftoff.

The equations of motion and impact equations were derived using the TMT method[25] and independently verified using Lagrangian mechanics and conservation of angular momentum; the resulting equations are far too long to be included in this paper. Integration of the equations is performed using MATLAB's `ode45()` function with absolute and relative tolerances of 10^{-5}.

2.2.2. Control of realistic model. The swing-leg retraction rate is defined as the angular velocity of the "virtual leg," that is, the line connecting the hip and the foot. This swing-leg retraction is not to be confused with swing-leg contraction, which is the time derivative of the length of the virtual leg. Although both swing-leg retraction and swing-leg contraction are required for perfect ground speed matching (and zero impact loss), the swing-leg contraction rate at touchdown is set to zero because humans tend to exhibit much more swing-leg retraction than swing-leg contraction[5] and the physical Phides robot does not permit swing-leg contraction when the stiff leg spring is engaged shortly before touchdown.

During the flight phase, all joints are proportional-derivative (PD)-controlled to follow quadratic spline trajectories that minimize maximum acceleration magnitudes. During the last part of the flight phase, the swing-leg knee joint is locked and the hip joint rotates with a constant angular rate ω. During the stance phase, the hip and the knee joint of the swing leg follow quadratic spline trajectories as during the flight phase. The only control of the stance leg is a torque at the knee during the second half of the stance phase, from maximal knee compression to liftoff, which attempts to regulate the system energy.

2.2.3. Simplified impact equations. In addition to the realistic model, we use a simplification of the realistic model to study the effects of swing-leg retraction on the impact event (Fig. 5). In the simple kneed leg model, the touchdown leg is entirely preserved, but the other leg and the torso are lumped

Table I. Parameter values of the realistic model and physical robot. See Fig. 4 for the parameter definitions, in which parameters are given by the property symbols with a subscript indicating the segment. The parameters of the simplified models are determined by combining or lumping segment masses as appropriate.

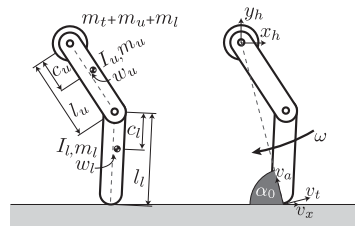|	Torso	Upper leg	Lower leg
Mass, m (kg)	7.41	2.54	0.51
Moment of inertia, I (kgm^2)	–	0.036	0.005
Length, l (m)	–	0.3	0.3
Vertical offset CoM, c (m)	–	0.183	0.139
Horizontal offset CoM, w (m)	–	0	0

Fig. 5. Kneed leg model, a simplification of the realistic model in which the mass of the opposing leg and the torso are lumped into a point mass at the hip.

into a point mass at the hip. The equations are derived and used in a similar fashion as the simplified prismatic leg model.

2.3. Physical robot

2.3.1. Hardware. We use the physical running robot Phides, shown in Fig. 1 with parameters tabulated in Table I, to validate our models. The robot is attached to a parallelogram boom to achieve approximately planar behavior, and the rotation of the torso is fixed with respect to the boom to eliminate the need to control the torso angle. Leaf springs, torsion bars, and a nonlinear transmission implement an effective prismatic (i.e. telescoping, as opposed to rotary) spring of constant stiffness between the foot and the hip, as in the SLIP and realistic models, during stance. An end stop prevents the knees from extending beyond the rest length of the parallel spring. Contact sensors in the feet, digital encoders with resolution 2×10^{-4} rad at the knees and boom, and encoders with resolution 6×10^{-5} rad at the hips measure the full state of the robot.

2.3.2. Control of robot. The controller of the robot is similar to the controller of the realistic model. However, communication delays and limited sensor accuracy on the robot limit the gains of PD-controllers, limiting the accuracy to which the quadratic spline joint trajectories are tracked. This inaccuracy makes it difficult to set the swing-leg retraction rate to a desired level; instead we measure the touchdown angle and flight time over a large number of steps and consider the effective retraction rate to be the slope of a linear least-squares fit through the data.

The robot uses a different push-off strategy than the realistic simulation model because the knee actuators are not capable of injecting sufficient energy during the second half of the stance phase alone. To deliver more energy into the system, the knee actuator tensions the leg spring before touchdown and applies a constant, maximal torque in the same direction as the knee angular velocity during the first half of stance.

3. Impact Losses

Swing-leg retraction rate affects the energy usage of running systems. The most obvious reason is that the speed of the foot, and thus the energy loss as the foot impacts the ground, is greatly influenced by the swing-leg retraction rate. While there are other sources of losses in running, we will first investigate the effect of swing-leg retraction on the impact losses of the realistic model given
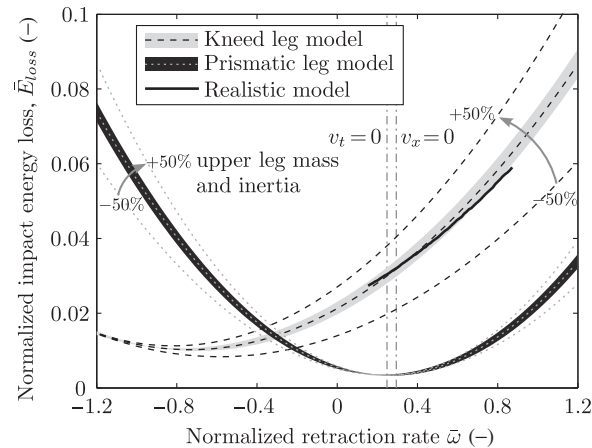
Fig. 6. The effect of the normalized swing-leg retraction rate $\bar{\omega}$ on the normalized energy loss $\overline{E}_{loss}$ for a prismatic leg model, kneed leg model, and realistic model. For each model, this is calculated as the difference between the energy of the model immediately before and after impact. For the simplified models, shaded regions indicate results for a range of touchdown conditions, including variations in instantaneous velocity and angle of attack, encountered at touchdown in limit cycles of the realistic model. Lines indicate the mean result for the range of touchdown conditions studied.

in Section 2.2 and the two simplified impact models given in Sections 2.1.3 and 2.2.3 to test our intuition regarding the most apparent link between swing-leg retraction and efficiency.

3.1. Methods
Impact losses are determined by taking the difference between the kinetic energy of the system immediately before and immediately after the instant of touchdown. The impact losses of the realistic model are determined while running under the hand-tuned controller in Section 2.3.2. All elements of the realistic model touchdown states except for retraction rate are mapped onto the prismatic and kneed leg models. To investigate the sensitivity of impact loss with respect to typical state variations, impact loss is calculated for the simplified models in all of these touchdown states for a variety of retraction rates. In order to investigate the sensitivity of the results for the prismatic and kneed leg models with respect to parameter variations, impact losses are calculated for the models with $\pm 50\%$ upper leg mass.

3.2. Results
Figure 6 shows the effect of the swing-leg retraction rate on impact loss of prismatic and kneed legs for a range of typical touchdown states and varying upper leg masses. For the prismatic model, the curves agree very closely; all have a minimum at the retraction rate that zeros the foot tangential speed, in agreement with previous results[14] that energy loss is minimized when the tangential component of the foot speed v_t is zero. Note that this is not, in general, the same as zeroing the horizontal component of the relative velocity between the foot and the ground, v_x. The location of minimal impact loss for the kneed leg is very different from the normalized retraction rate for zero foot tangential speed and depends on the mass distribution of the leg. The results of the realistic model are superposed and show close agreement with the simplified kneed leg model.

3.3. Discussion
Figure 6 shows that variations within the characteristic range of touchdown horizontal speeds, touchdown vertical speeds, and angles-of-attack have little effect on the normalized energy loss, as indicated by the narrow bands. Also, for prismatic legs, mass distribution of the leg has little effect on the trend, as the minima of the lines for $\pm 50\%$ upper leg mass share a minimum with the band for normal robot mass parameters.

For kneed legs, however, the minima of the curves lie at a much lower retraction rate than that of zero horizontal or tangential speed. That is, our intuition about lower impact loss stemming from reduced relative speed between the foot and the ground, or ground speed matching, does not hold for

kneed legs when there is no swing-leg contraction during flight. However, we can adjust our intuition by considering that the impact loss is not only due to abrupt changes in the translation of the foot or leg segments, but also due to abrupt changes in the rotation of leg segments. Note that immediately before touchdown, the rate of swing-leg contraction is very low (by constraint), but immediately after touchdown, there must be significant leg contraction as the knee bends. This sudden increase in leg contraction is manifested as a decrease in the angular velocity of the upper leg segment and an increase in the angular velocity of the lower leg segment. The impact losses due to these sudden jumps in angular velocity are lower if the more massive upper segment has a less positive, or even more negative, angular velocity prior to touchdown. Indeed, the minima of the impact loss curves for the kneed leg models occur at much lower retraction rates than for prismatic leg models. Furthermore, the more massive the upper leg segment, the more pronounced is this effect: as upper leg mass is increased, the retraction rate at which the minimum occurs is decreased.

The curves for a kneed and prismatic leg are quite different, so we cannot consider the prismatic leg a representative simplification of a kneed leg when studying impact losses. This suggests that while the results of Haberland *et al.*[18] may be valid for prismatic legged robots, they do not necessarily generalize to kneed legs as originally suspected. On the other hand, the kneed leg model agrees closely with the realistic model, indicating that the state of the second leg of the realistic model at impact does not significantly affect the energy loss.

4. Overall Energetic Efficiency

Impact loss is not the only factor in running energetic efficiency; another consideration is that the forward and rearward acceleration of the swing leg is accomplished, at least in part, by actuator work, and thus the swing-leg retraction rate is the result of a certain energy expenditure. Perhaps subtler still is that the state of the leg as it touches down sets the initial conditions for the stance phase, during which much of the work of running is done, and the ensuing dynamics is significantly affected by the initial conditions. Since impact losses are only a portion of the energy expenditure of the robot in running, it is unclear *a priori* whether the reduction in impact loss due to a given retraction rate leads to an overall efficiency improvement. Therefore, we consider the effect of the retraction rate on overall limit cycle energetic efficiency of the Phides robot in simulation.

4.1. Methods

We measure the overall energetic efficiency of the realistic model of Section 2.2 in limit cycle motion for a range of swing-leg retraction rates. We quantify the energy efficiency using mechanical cost of transport c_{mt}, which is the energy consumed by the actuators normalized by the robot's weight and distance traveled. The energy consumed is assumed to be the integral of the absolute mechanical power of the actuators. Thus,

$$c_{mt} = \frac{\int_0^{t_{step}} |\tau \cdot \dot{\phi}| \, dt}{M \cdot g \cdot x_{step}}, \tag{1}$$

in which t_{step} is the temporal duration of a step, x_{step} is the distance traveled in a step, τ is the vector of instantaneous joint torques, $\dot{\phi}$ is the vector of the angular velocities of the joints, M is the total robot mass, and g is the gravitational acceleration.

4.2. Results

Figure 7 shows the effect of swing-leg retraction rate on efficiency. While the optimal efficiency is found at a normalized retraction rate of 0.4, the absolute effect of the retraction rate on the cost of transport is small, with a maximal difference of only 5% over the whole range of retraction rates.

4.3. Discussion

Although Fig. 6 in Section 3 showed a pronounced effect of swing-leg retraction rate on impact losses, Fig. 7 shows very little effect of swing-leg retraction rate on mechanical cost of transport. In fact, even when we computed the cost of transport of optimally efficient limit cycles as a function of swing-leg retraction rate in another study,[26] we found the same trend: swing-leg retraction has little effect on overall energetic efficiency. This is surprising, because it seems intuitive that increased
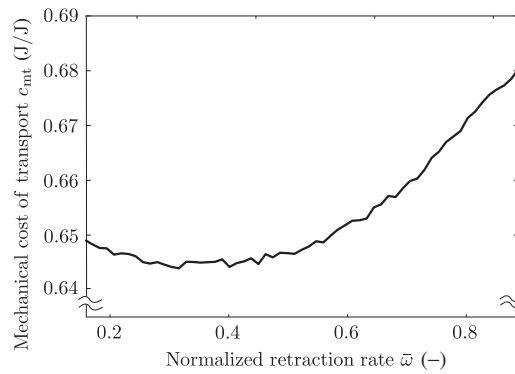
Fig. 7. The effect of the normalized retraction rate $\bar{\omega}$ on the mechanical cost of transport of limit cycle running under the hand-tuned controller.

impact losses would result in lower efficiency,[17] and a previous work[18] showed correlation between impact loss and minimal mechanical cost of transport; however that was for a simulated machine with prismatic, rather than rotary-kneed, legs.

To consider why this is so, recall that the efficiency, as measured by cost of transport, is the ratio of robot's energy expenditure to the product of its weight and distance traveled. The robot's energy expenditure can be broken down into three components: the energy loss at impact, the energy required to swing the legs, and the energy required to produce the vertical impulse. We have observed that swing-leg retraction has a strong effect on the component of energy expenditure due to impact losses, yet has little impact on net efficiency. Therefore, the combined effects of swing-leg retraction on the other two components of energy expenditure and distance traveled must almost exactly oppose and thus approximately nullify the effects on impact loss. This is a very unexpected result, as these other effects are far less intuitive than the effects on impact loss, and it highlights the importance of performing calculations with a complete model rather than assuming that partial results from heavily simplified models will scale to models of higher complexity.

5. Impact Forces and Footing Stability

When designing a robot controller, it may be necessary to minimize the magnitude of impact forces at touchdown to avoid damaging the robot, and it is often important to limit sliding between the foot and the ground to avoid slipping and falling. By changing the relative speed between the foot and the ground at touchdown, swing-leg retraction can have a significant effect on the extent to which these risks are mitigated. In this section, we analyze the effect of swing-leg retraction on impact forces and slippage.

5.1. Methods

The realistic model and the two simplified impact models are not appropriate for predicting the magnitude of touchdown forces because touchdown is modeled as an instantaneous event with impulses rather than finite forces. However, we can assume that the risk of damage is roughly proportional to the magnitude of the touchdown impulse. Likewise, the simulation does not predict how much slipping will occur at touchdown because the foot is assumed to stick to the point of ground contact. However, we can assume that slipping at touchdown will depend on the angle of the touchdown impulse: If the impulse angle is zero, the impulse is purely vertical, and slipping is impossible; if the impulse angle is $\pi/2$, the impulse is purely horizontal, and slipping is certain. At intermediate angles, slipping will occur if the impulse angle exceeds the effective friction angle, the arctangent of the effective friction coefficient. The magnitude and angle of the impulse vector are computed similarly to the impact energy loss, detailed in Section 3.1.

5.2. Results

Figure 8 shows the magnitude of the touchdown impulse as a function of the retraction rate for prismatic leg, kneed leg, and realistic models. For the prismatic leg, the magnitude of the touchdown
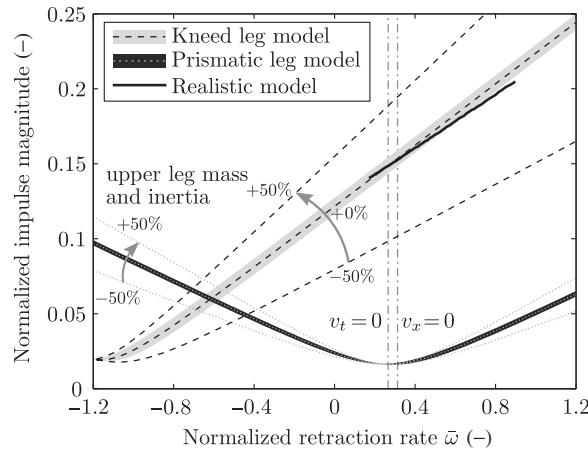
Fig. 8. The effect of the normalized swing-leg retraction rate $\bar{\omega}$ on the normalized touchdown impulse magnitude for prismatic leg, kneed leg, and realistic models. The meaning of strokes and shading are the same as in Fig. 6.
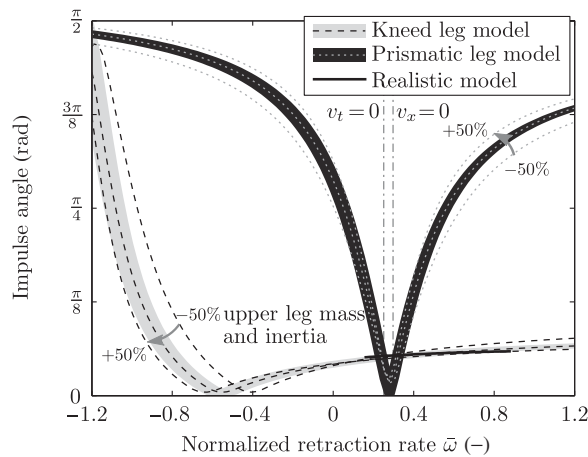

Fig. 9. The effect of the normalized swing-leg retraction rate $\bar{\omega}$ on the impulse angle for prismatic leg, kneed leg, and realistic models. Impulse angle, or the magnitude of the angle between the impulse and vertical, is defined as $|atan(I_x/I_y)|$, where I_x and I_y are the horizontal and vertical components of the impulse vector respectively. A lower value corresponds with an impulse closer to vertical and less slipping at touchdown. The meaning of strokes and shading are the same as in Figs. 6 and 8
.

impulse is minimal at the retraction rate for which foot tangential speed is zero, as anticipated by analysis presented in Karssen *et al.*[14] However, the minimal touchdown impulses for the kneed leg occur at negative retraction rates very different from the retraction rate of zero foot tangential speed. Again, the realistic robot model shows close agreement with the simplified kneed leg model.

Figure 9 shows the angle of the touchdown impulse as a function of the retraction rate. The larger the angle, the more likely that slipping will occur. For the prismatic leg, the retraction rate has a large influence on the impulse angle and the minimal angle occurs near the retraction rate for which the foot tangential speed is zero. For the kneed model, however, the retraction rate has a much smaller effect on the impulse angle. For all normalized retraction rates between −0.8 and 1.2, the impulse angle is low enough so that an effective friction coefficient of 0.2 would be sufficient to prevent slipping. Also for the impulse, the realistic robot model shows close agreement with the simplified kneed leg model.

5.3. Discussion
Many conclusions analogous to those about impact losses in Section 3.3 can be drawn from Figs. 8 and 9. However, there is also a new trend that the impulse angle observed for the prismatic leg rises
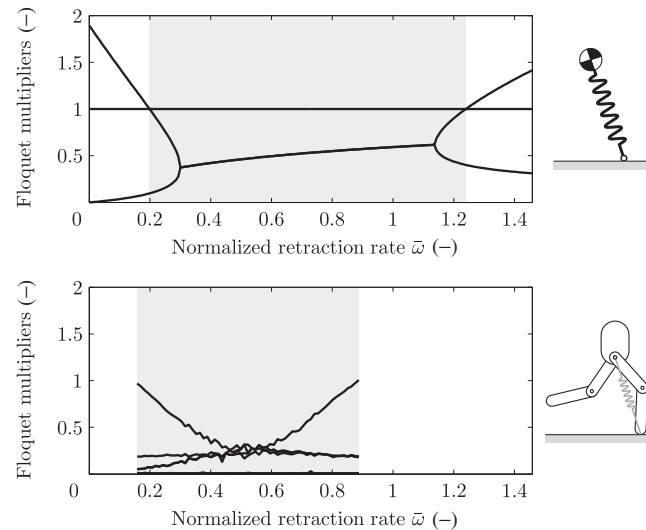
Fig. 10. Floquet multipliers as functions of normalized retraction rate for both SLIP and realistic models. The gray areas indicate the range of normalized retraction rates for which the models are stable.

very sharply from the minimum, but the impulse angle of the kneed leg model is not very sensitive to retraction rates greater than the optimum. Thus, for the prismatic leg, the foot tangential speed must be almost precisely zero to avoid slipping, but the kneed leg is unlikely to slip for a wide range of swing-leg retraction rates. For example, with a coefficient of friction being 1 between a rubber robot foot and concrete, slipping will occur at an impulse angle greater than $\arctan 1 = \pi/4$. Consequently, for the prismatic leg model, the normalized retraction rate must be within ± 0.3 of that required for $v_t = 0$ to prevent slipping. For the kneed leg, on the other hand, slipping is unlikely for all but the most negative retraction rates. This may be an inherent advantage of a rotary knee over a telescoping joint.

6. Stability
In Seyfarth *et al.*,[12] swing-leg retraction is introduced as a simple control strategy to improve stability, or small disturbance response, of the SLIP model. In this section, we assess how the retraction rate influences the stability of SLIP and realistic models.

6.1. Method
The stability of a running model can be assessed by analyzing the Floquet multipliers of its step-to-step behavior,[12,27] that is, the eigenvalues of the linearized, discrete step-to-step map A. The map A governs the dynamics of perturbations from limit cycles $\Delta\mathbf{v}_i$ as

$$\Delta\mathbf{v}_{n+1} = A\Delta\mathbf{v}_n \quad \text{with } \Delta\mathbf{v}_n = \mathbf{v}_n - \mathbf{v}^*, \tag{2}$$

in which $\mathbf{v}_i$ is the state of the system at a specific point in the gait cycle (e.g. state at liftoff) of the ith step and $\mathbf{v}^*$ is the state at this point in the limit cycle. The Floquet multipliers indicate the rate at which the model converges back to the limit cycle after a small deviation from the limit cycle. A system is stable if the magnitude of all Floquet multipliers is less than unity.

6.2. Results
Figure 10 shows how the magnitude of the Floquet multipliers varies across a range of retraction rates for SLIP and realistic models respectively. The Floquet multipliers for the realistic model are shown only for retraction rates for which the model has a stable limit cycle, as our method for finding limit cycles requires the model to be stable.

The SLIP model has three Floquet multipliers, as the state at apex can be described by three state variables: apex height, horizontal speed, and leg angle. Due to the energy conservative nature of the

SLIP model, one of the Floquet multipliers is always unity, signifying that disturbances to energy level persist. We neglect the technicality that this trivial eigenvalue precludes stability in the strictest sense, and refer to any marginally stable limit cycles of the SLIP as stable.

The magnitude of the other two Floquet multipliers is less than unity for normalized retraction rates between 0.20 and 1.24. Outside this range, one of the Floquet multipliers has a magnitude greater than unity, which means that the limit cycle running is unstable at these retraction rates. The convergence rate is maximal at a normalized retraction rate of 0.30, where the largest magnitude of the two nontrivial Floquet multipliers is minimal.

The realistic model has eight Floquet multipliers, as the state at touchdown can be described by eight state variables corresponding to the angle and the angular rate of upper and lower segments of both stance and swing leg. Four of the Floquet multipliers are almost zero over the range of retraction rates, which is due to the stiff position control of knees. The realistic model is stable for normalized retraction rates between 0.15 and 0.89. Within this range of stable retraction rates, a normalized retraction rate of 0.46 results in the fastest convergence rate.

6.3. Discussion

Both models show that the retraction rate affects the stability. However, the models show different ranges of retraction rates for which the model is stable. The lowest retraction rate of about 0.2 at which the model is stable is the same for both models. On the other hand, the highest retraction rate at which the model is stable is 1.24 for the SLIP model and only 0.89 for the realistic model. In addition, the trend of the largest nontrivial Floquet multiplier differs between the models. For the SLIP model, this Floquet multiplier is nearly constant over most of the range of stable retraction rates, while for the realistic model it varies from a maximum of unity at the boundaries of the range of stable retraction rates to 0.3 at the center of the interval. This highlights the importance of performing stability analysis on realistic models, and suggests that the SLIP model is not very suitable for studying the effects of swing-leg retraction on stability; it cannot be used to select the retraction rate for optimal stability of realistic models or physical robots.

7. Disturbance Rejection

Besides affecting the stability with respect to infinitesimal disturbances, swing-leg retraction also affects the response to large disturbances. In this section, we quantify how the large disturbance rejection of simple SLIP and realistic models is influenced by the swing-leg retraction rate.

In the field of legged robots, many ways to quantify the rejection of large disturbances have been proposed,[28,29] but there is little agreement on a standard. In this paper, we show the effect of swing-leg retraction on three disturbance rejection measures: *settling time*, *maximal single relative disturbance*, and *mean steps to fall*. These were selected because they are intuitive measures of how well a robot can handle real-world disturbances and because their computational costs are not excessive.

7.1. Method

The *settling time* is the time that a system takes to return to a steady gait after a disturbance.[30] For running systems, it is important to return to a steady gait quickly; the slower the convergence, the more likely for successive disturbances to move the system progressively further from the limit cycle to failure. The return to a limit cycle is measured using a gait indicator, a quantitative characteristic of the gait that, when outside a normal range, is observed to correlate with failure. We use step time as a gait indicator because it has been observed that large deviations in step time tend to correlate with subsequent failure.[28,31] We define the settling time as the number of steps after a disturbance before the step time is within 0.1% of its steady state value. As the disturbance, we use an energy-neutral step-down: in addition to a step in ground height, the forward speed is adjusted to keep the system energy constant. This disturbance is chosen because it allows the energy conservative SLIP model to return to the original limit cycle. The step-down is chosen to be 3.5% of the leg length, as this disturbance did not cause either model to fall for a wide range of retraction rates.

The *maximal single relative disturbance* is the maximum change from a known limit cycle state from which the robot will not fall within a prescribed number of steps.[32–34] This measure gives an

indication of the size of the basin of attraction, which is the collection of all initial states that do not lead to a fall. We consider two types of single relative disturbances:

- A push disturbance is an increase (push forward) or decrease (push backward) from a known limit cycle apex hip velocity. This is equivalent to the application of an impulse uniformly distributed over the mass of the robot.
- A step disturbance is an increase (step-down) or decrease (step-up) from a known limit cycle apex hip height. This is equivalent to a single step in the floor over which the robot is running.

The maximal single relative disturbance is determined by applying increasingly large disturbances until the model falls within 25 steps of the disturbance.

The *mean steps to fall* metric is inspired by a measure of manufacturing system reliability known as mean time to failure.[35] Mean steps to fall is defined as the average number of steps, starting from a given limit cycle, before a robot falls under the influence of a sequence of finite disturbances randomly sampled from a given distribution. We consider both absolute step disturbances, or normally distributed perturbations in the apex vertical height above mean ground level, and absolute push disturbances, or normally distributed perturbations in the apex horizontal speed. Mean steps to fall are estimated by measuring the number of steps to fall over 100 different sequences of disturbances randomly sampled from a Gaussian distribution with zero mean and specified standard deviation, then averaging across all trials.

For SLIP and realistic models, the most obvious fall mode is when the hip touches the ground. However, we define two additional fall modes for the realistic model: when the swing foot touches the ground (trip), and when the model touches down with the stance leg bent further than the rest length of the leg spring permits. It is necessary to enforce this condition as a fall to prevent the leg spring from engaging at a non-zero energy level. The robot Phides has a similar fall mode, because its leg spring only engages at the spring rest length; the leg will collapse if the rest length is not reached before touchdown.

7.2. Results

Figure 11 shows the settling time as a function of the retraction rate for the two models. In addition, it shows the response of the gait indicator for three retraction rates. For low retraction rates, the gait indicator slowly converges to its steady state value. With increasing retraction rates, the convergence rate increases and settling time decreases. If the retraction rate is increased too much, the gait indicator overshoots and oscillates about its steady state value. The two models show this effect of retraction rate on the settling behavior, but the ranges of retraction rates for which each behavior occurs differ between the models.

Figure 12 shows the maximal single step and the maximal push disturbance for a range of retraction rates for the two models. The effect of the retraction rate on the maximal single relative disturbance seems to differ between disturbances that add energy and remove energy. For disturbances that remove energy from the system, such as the step-up and the backward push, the maximal disturbance increases with increasing retraction rate until the retraction rate for which the system becomes unstable. On the other hand, for disturbances that add energy to the system, such as the step-down and the forward push, the maximal disturbance peaks at a lower retraction rate, especially for the SLIP model.

While both models reveal that retraction rate greatly affects the maximal single relative disturbance, there are large quantitative differences. For example, the maximal step-up that the realistic model can handle is about two times as large as what the SLIP model can handle. In fact, the only quantitative agreement between the two models is that for maximal forward push, both models achieve maximal disturbance at a normalized retraction rate of about 0.55–0.6, but here the peak for the SLIP model is sharply defined whereas for the realistic model the curve is relatively flat.

Figure 13 reveals a substantial effect of the retraction rate on the mean steps to fall. With a normalized retraction rate of 0.33, the realistic model rejects step disturbances for an average of 124 steps, where with a retraction rate of 0.63 it only averages 21 steps. It is interesting that the maximal mean steps to fall for the step disturbances occur at nearly the same retraction rate for maximal mean steps to fall with push disturbances. This holds for both SLIP and realistic models, but the optimal retraction rate for the SLIP model is at a much higher retraction rate than the optimal retraction rate of
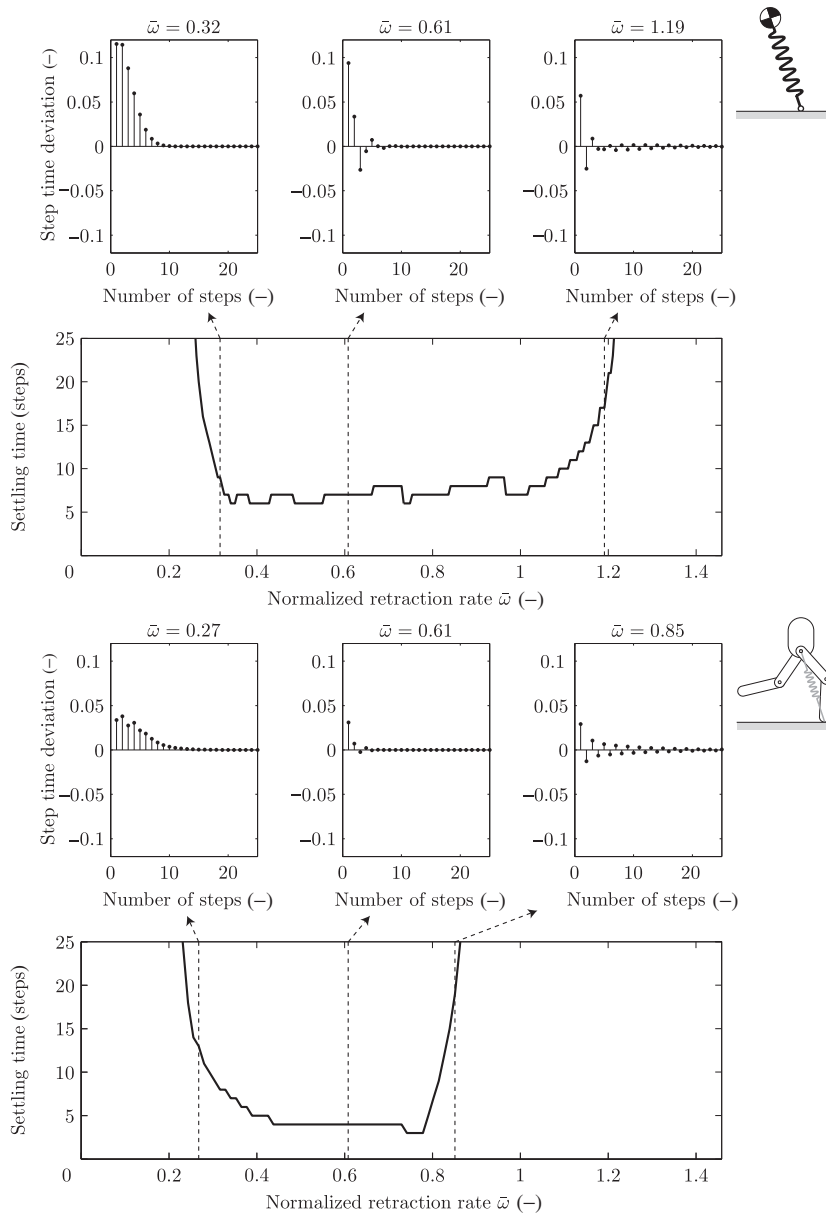
Fig. 11. The settling time as a function of the retraction rate for the two simulation models. The settling time indicates how quickly the system returns to a steady gait after a disturbance. An energy-neutral step-down 3.5% L_0 was used as disturbance. The inserts show the response of the gait indicator, step time, after a disturbance for three retraction rates. At low retraction rates there is slow convergence, at medium retraction rates there is quick convergence, and for high retraction rates there is an oscillating convergence.

the realistic model. Also, the value of maximum mean steps to fall with push disturbances is several times higher for the realistic model than for the SLIP model.

7.3. Discussion

There is an interesting correlation between settling time and stability. For instance, the SLIP model has a substantially wider range of retraction rates for which the settling time is very low, or less than five steps, than the realistic model. This reminds us of SLIP's wide range of low, nearly constant, maximal, nontrivial eigenvalue. Also, the range of retraction rates in which the settling time is reasonable, or less than 25 steps, corresponds with the ranges for which the models are stable.

All three measures show that swing-leg retraction has a large influence on the disturbance rejection behavior for the SLIP as well as realistic model. However, the trends are different for the three
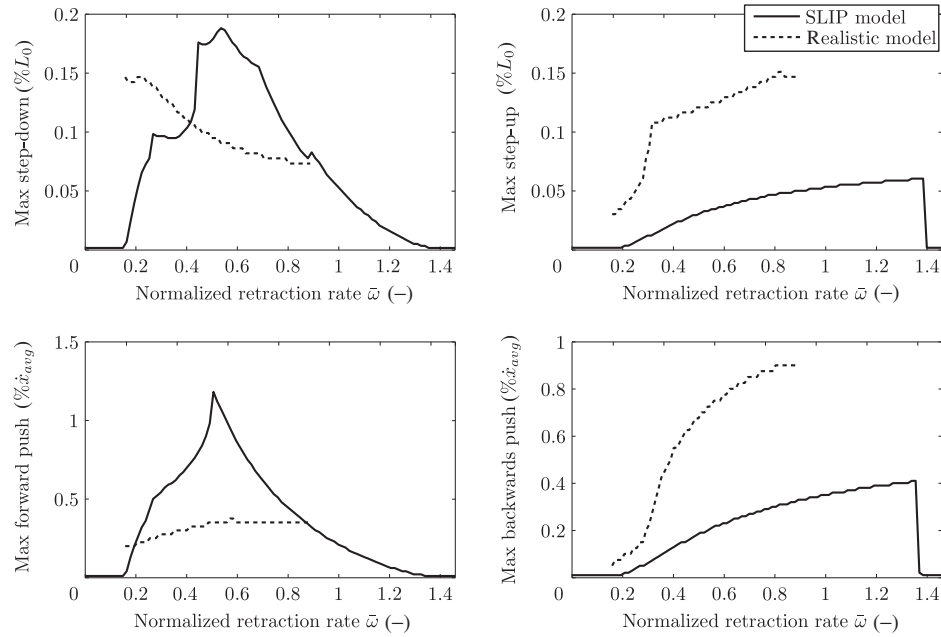
Fig. 12. The maximal single relative disturbance as a function of the normalized retraction rate of SLIP and realistic models. Four kinds of disturbances are used: step-down (top left), step-up (top right), forward push (bottom left), and backward push (bottom right).
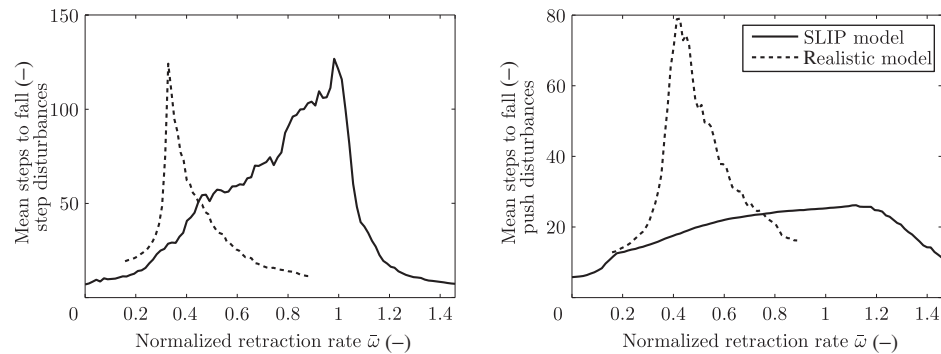

Fig. 13. The effect of retraction rate on the mean steps to fall for both simulation models. The mean steps to fall are shown for random step disturbances with a standard deviation of 2.6% L_0 (left) and push disturbances with a standard deviation of 15% $\dot{x}_{\text{avg}}$ (right).

measures and are dependent on the kind of disturbance used. This indicates that if swing-leg retraction is implemented to increase disturbance rejection, the retraction rate should be chosen based on expected disturbances; it cannot be chosen to maximize rejection of all disturbance types at once.

Comparing the result of the SLIP model with that of the realistic model, we can see that the models qualitatively agree on some of the disturbance rejection measures, such as settling time, maximal step-up, and backward push. However, there is no agreement on other disturbance rejection measures such as the mean steps to fall. In addition, there is no quantitative agreement for any of the measures, which means that the SLIP model cannot be used to select the optimal retraction rate for realistic robot models or robots.

8. Discussion

8.1. Realistic model validation

The realistic model used in this paper is based on the running robot Phides. To test the validity of the realistic model, we compare its behavior with the robot's behavior at a normalized retraction rate
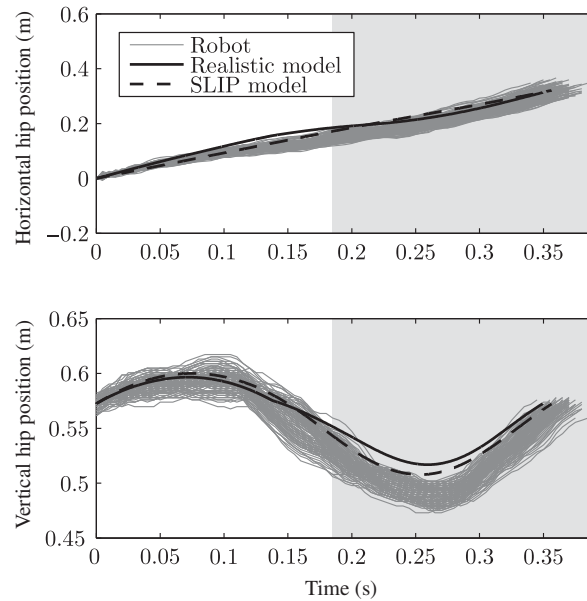
Fig. 14. Comparison of hip trajectory of the SLIP model, realistic model and the robot, all with a normalized retraction rate of 0.62 and running at a normalized speed of 0.38. The robot's hip trajectory is of 108 consecutive steps, with the horizontal hip position defined to be zero at liftoff. The white areas indicate the average duration of the flight phase of the robot and the gray areas indicate the stance phase.

of 0.62. For completeness, we also include the SLIP model in this comparison. First, we compare the hip trajectories as shown in Fig. 14. There is a close agreement between the hip trajectory of the models and the robot, which suggests that they have similar limit cycles.

For the experiments in this paper, it is important that, besides having similar limit cycles, the model and the robot respond similarly to disturbances. Figure 15 shows the response to a relative step-up disturbance of 5% L_0 of both models and the robot. The realistic model and the robot have similar responses in the steps following the disturbance: a decrease in step time, an increased in step time, finally convergence back to the nominal step time. The SLIP model, on the other hand, responds with a sequence of two short steps, a long step, a short step, and then failure. This shows that the SLIP model does not capture the disturbance response of the physical robot well, while the realistic model does.

Based on these two comparisons, we believe that the realistic model is valid, and that the effects of swing-leg retraction on the realistic model transfers over to the robot. To further validate the results of this study, we would implement additional swing-leg retraction rates and measure all the performance metrics addressed in this paper.

8.2. Effect of controller implementation

For the robot and the realistic model, we selected a particular hand-tuned feedback controller based on a variety of criteria: disturbance rejection behavior, ease of implementation, ease of tuning, compatibility with swing-leg retraction, etc. This controller is not uniquely suitable for this study, and results obtained are not necessarily applicable to other robots using different controllers. However, testing the robot with this controller gives us an initial indication of how performance criteria are affected by swing-leg retraction rate; it is the first step in the general understanding of the effects of swing-leg retraction. If in the future similar tests are performed using other controllers and similar results are obtained, it may be assumed that these effects are general and hold for most controllers. Alternatively, if the results of other controllers are very different, this can lead to an interesting conclusion that the effects of swing-leg retraction are highly dependent on specific aspects of controller implementation.

Note that in a previous study[26] we began to explore the effect of swing-leg retraction on the overall energetic efficiency in a manner that is, in some sense, independent of a particular controller. In that study, we measured the effect of swing-leg retraction on the cost of transport of (locally) *optimal*
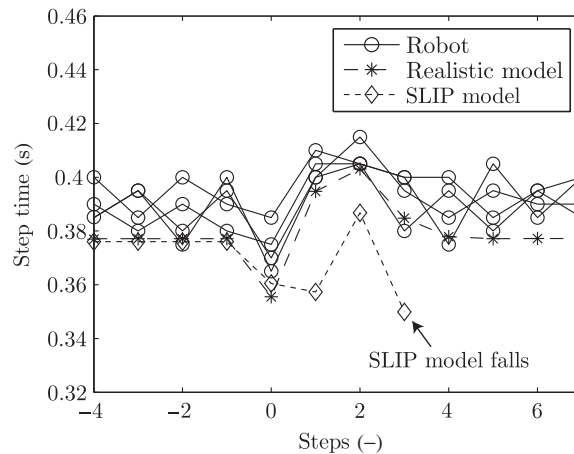
Fig. 15. The response in step time, measured from liftoff to liftoff, of the SLIP model, realistic model and the robot on a relative step-up disturbance of 5% L_0 while running at a normalized speed of 0.33. The robot response is shown for four separate trials. The step time of the robot is measured with a resolution of 5 ms. The robot and the realistic model show a decrease in step time at the step-up followed by an increased step time for the following steps. The SLIP model has a different response in step time and falls in the fourth step after the disturbance.

gaits, and thus established an approximate lower bound on cost of transport to which robots with other efficient controllers can be compared. As mentioned previously, we found that the results were consistent with those of the present study.

8.3. Are the trends of the models consistent?
This question has been discussed separately for the different performance metrics in Sections 3.3, 5.3, 6.3, and 7.3. Following is the summary:

- The SLIP model correctly predicts that a modest swing-leg retraction rate will improve both stability and disturbance rejection, and it correctly identifies the shape of many trends in a qualitative sense. However, because it does not make an accurate quantitative prediction of the location of extreme points for any curve, it cannot be used to predict whether increasing the retraction rate from a certain positive value will improve or degrade stability or disturbance rejection.
- The prismatic leg model does not predict the trends observed in the realistic model for impact loss, impulse magnitude, or impulse angle; in all of these cases, it even gets the direction of the optimal retraction rate wrong.
- The kneed leg model correctly predicts the trends observed in the realistic model for impact loss, impulse magnitude, and impulse angle.

One might argue that it is obvious that the results of the prismatic leg model would not agree with the realistic model due to fundamental differences in their morphology. But clearly, differences in morphology cannot always preclude agreement between simple models and realistic models or physical robots, or it is unlikely that the SLIP model would be such a popular model in the literature. Because it is difficult to assess *a priori* and on intuitive grounds whether a given model simplification will accurately predict trends of a more realistic model, we believe it is important to study realistic running models in conjunction with simple models. Simple models may be used to help identify new phenomena or explain known behaviors, but in either case the extent of agreement with more realistic models must be studied in order for the results to be most useful for application to running machines.

8.4. Optimal retraction rate
In this paper, we investigated the effect of the swing-leg retraction rate on the following six performance metrics: impact losses, cost of transport, impact forces, the risk of slipping, stability, and disturbance rejection. The retraction rate has a substantial effect on all but one of these performance metrics, namely the cost of transport, for which the maximal effect is less than 5%. For all the other studied performance metrics, there is a substantial improvement by swinging the leg at a
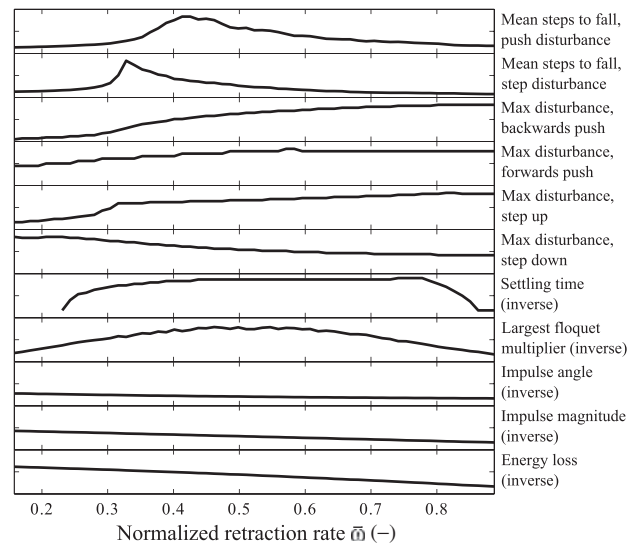
Fig. 16. The effect of swing leg retraction rate on all performance metrics for the realistic model running at normalized average horizontal speed of 0.42. Metrics for which lower values are better have been inverted (negative) so that the the optimal value corresponds with the *maximum* of each plot. All axes are scaled between 0 and the most extreme value of the metric.

non-zero retraction rate compared with no retraction. However, the maximal improvement for each performance metric is found at a different retraction rate. For the realistic model, there are even performance metrics that require a negative retraction rate for optimal performance. This presents a trade-off when selecting the retraction rate, which is in agreement with Karssen *et al.*[14]

The results of this paper also showed that the effect of swing-leg retraction is very dependant on leg morphology, especially for the performance metrics that are strongly affected by the touchdown dynamics. For a kneed leg morphology, the mass distribution also affects the effect of swing-leg retraction. As a result, we cannot recommend any simple formula for selecting an overall optimal retraction rate. If the control system is designed such that retraction rate is a relatively independent parameter, the "optimal" retraction rate will likely depend on the specific design of the robot, the particulars of the rest of the control system, and the relative importance of different performance metrics. The retraction rate should be chosen accordingly, based on simulation and experiment.

Figure 16 summarizes all the results obtained using the realistic model and is useful for selecting the optimal retraction rate. For Phides, we are not interested in demonstrating energetic efficiency, we have not noticed severe problems with slipping at impact, and there are no particular concerns about impact forces damaging the robot. We believe that Phides' greatest contribution would be in the area of robustness against typical real-world disturbances such as an uneven floor, so we would choose a moderate positive retraction rate near $\bar{\omega} = 0.4$, which is a compromise among low maximum eigenvalue magnitude, low settling time, and high mean steps to fall under random step disturbances. Under this controller, the robot would exhibit quick recovery and few falls when subjected to the perturbations of common outdoor terrain such as asphalt, sidewalks, and low grass.

9. Conclusions

In this paper, we showed how the benefits of swing-leg retraction depend on the retraction rate for simple and realistic mathematical models validated against a physical robot. Based on these results we conclude the following for the kneed leg morphology and parameters used in this study:

- Swing-leg retraction can be used to decrease the impact energy loss, but the overall effect on efficiency, as measured by mechanical cost of transport, is small.
- Swing-leg retraction can decrease touchdown forces and increase footing stability, as estimated by impact impulses.

- Swing-leg retraction can increase several measures of stability and disturbance rejection, and can, to a limited extent, increase all measures simultaneously.
- The optimal retraction rate depends heavily on the metrics of running performance that are valued and the specifics of the systems; generalizations are difficult to generate.

   More generally, we conclude the following:

- A prismatic leg is not a satisfactory simplification of a kneed leg when considering the touchdown impact event; the impact dynamics of the two models is fundamentally different.
- The SLIP model may be a useful template for the prediction of running behaviors such as hip trajectories,[19] but it is not a satisfactory simplification of a general running robot for the study of some complex behaviors such as stability and disturbance rejection.
- Indeed, such relationships may defy general trends as they are strongly dependent on the robot morphology, parameters, and controller. Robot designers must use accurate models of their own machines to predict the effect of swing leg retraction on these behaviors.

References

1. M. Raibert, K. Blankespoor, G. Nelson, R. Playter and the BigDog Team, "Bigdog, the Rough-Terrain Quadruped Robot," *Proceedings of the 17th World Congress*, (2008) pp. 10823–10825.
2. U. Saranli, M. Buehler and D. E. Koditschek, "Rhex: A simple and highly mobile hexapod robot," *Int. J. Robot. Res.* **20**(7), 616–631 (2001).
3. S. Kim, J. E. Clark and M. R. Cutkosky, "iSprawl: Design and tuning for high-speed autonomous open-loop running," *Int. J. Robot. Res.* **25**(9), 903–912 (2006).
4. R. Müller and R. Blickhan, "Running on uneven ground: Leg adjustments to altered ground level," *Hum. Mov. Sci.* **29**(4), 578–589 (2010).
5. Y. Blum, S. W. Lipfert, J. Rummel and A. Seyfarth, "Swing leg control in human running," *Bioinspiration Biomimetics* **5**, 026006 (2010).
6. A. Seyfarth and H. Geyer, "Natural Control of Spring-Like Running: Optimized Self-Stabilization," *Proceedings of the Fifth International Conference on Climbing and Walking Robots* (2002) pp. 81–85.
7. M. H. Raibert, H. B. Brown, Jr., M. Chepponis, J. Koechling and J. K. Hodgins, "Dynamically stable legged locomotion," *Technical Report*, DTIC Document (1989). URL: http://www.dtic.mil/cgi-bin/GetTRDoc?Location=U2&doc=GetTRDoc.pdf&AD=ADA225713. Accessed February 13, 2014.
8. D. G. E. Hobbelen and M. Wisse, "Limit Cycle Walking," **In**: *Humanoid Robots, Human-like Machines* (M Hackel, ed.) (I-Tech, Vienna, Austria, 2007a) pp. 277–294.
9. F. Asano, "Effects of Swing-Leg Retraction and Mass Distribution on Energy-Loss Coefficient in Limit Cycle Walking," *Proceedings of the IEEE/RSJ International Conference on Intelligent Robots and Systems, 2009 (IROS 2009)* (IEEE, New York, 2009) pp. 3214–3219.
10. M. Wisse, C. G. Atkeson and D. K. Kloimwieder, "Dynamic Stability of a Simple Biped Walking System with Swing Leg Retraction," **In**: *Fast Motions in Biomechanics and Robotics*, (Moritz Diehl and Katja Mombaur, eds.), Lecture Notes in Control and Information Sciences, vol. 340 (Springer, Berlin, Germany, 2006) pp. 427–443. ISBN 978-3-540-36118-3. URL: http://dx.doi.org/10.1007/978-3-540-36119-0_21.
11. D. G. E. Hobbelen and M. Wisse, "Swing-leg retraction for limit cycle walkers improves disturbance rejection," *IEEE Trans. Robot.* **24**(2), 377–389 (2008).
12. A. Seyfarth, H. Geyer and H. Herr, "Swing-leg retraction: A simple control model for stable running," *J. Exp. Biol.* **206**(15), 2547–2555 (2003).
13. M. Ernst, H. Geyer and R. Blickhan, "Spring-Legged Locomotion on Uneven Ground: A Control Approach to Keep the Running Speed Constant," *International Conference on Climbing and Walking Robots* (2009) pp. 639–644.
14. J. G. D. Karssen, M. Haberland, M. Wisse and S. Kim, "The Optimal Swing-Leg Retraction Rate for Running," *Proceedings of IEEE International Conference on Robotics and Automation* (IEEE, New York, 2011) pp. 4000–4006.
15. F. Peuker, A. Seyfarth and S. Grimmer, "Inheritance of SLIP Running Stability to a Single-Legged and Bipedal Model with Leg Mass and Damping," *4th IEEE RAS & EMBS International Conference on Biomedical Robotics and Biomechatronics, 2012 (BioRob)* (IEEE, New York, 2012) pp. 395–400.
16. M. A. Daley and J. R. Usherwood, "Two explanations for the compliant running paradox: Reduced work of bouncing viscera and increased stability in uneven terrain," *Biol. Lett.* **6**(3), 418–421 (2010).
17. M. H. Raibert, *Legged Robots that Balance* (MIT Press, Cambridge, MA, 1986).
18. M. Haberland, J. G. D. Karssen, S. Kim and M. Wisse "The Effect of Swing Leg Retraction on Running Energy Efficiency," *Proceedings of IEEE/RSJ International Conference on Intelligent Robots and Systems* (IEEE, New York, 2011) pp. 3957–3962.
19. R. Blickhan, "The spring-mass model for running and hopping," *J. Biomech.* **22**(11), 1217–1227 (1989).

20. W. J. Schwind and D. E. Koditschek, "Characterization of Monoped Equilibrium Gaits," **In:** *Proceedings of IEEE International Conference on Robotics and Automation*, vol. 3 (IEEE, New York, 1997) pp. 1986–1992.
21. R. M. Ghigliazza, R. Altendorfer, P. Holmes and D. Koditschek, "A simply stabilized running model," *SIAM Revi.* **47**(3), 519–549 (2005). ISSN 00361445. URL: `http://www.jstor.org/stable/20453666`.
22. I. Poulakakis and J. W. Grizzle, "Modeling and Control of the Monopedal Robot Thumper," *Proceedings of IEEE International Conference on Robotics and Automation* (IEEE, New York, 2009) pp. 3327–3334.
23. R. Blickhan and R. J. Full, "Similarity in multilegged locomotion: Bouncing like a monopode," *J. Comp. Physiol. Neuroethol. Sens. Neural. Behav. Physiol.* **173**(5), 509–517 (1993).
24. R. J. Full and D. E. Koditschek, "Templates and anchors: Neuromechanical hypotheses of legged locomotion on land," *J. Exp. Biol.* **202**(23), 3325–3332 (1999).
25. R. Q. van der Linde and A. L. Schwab, "Multibody Dynamics B" (2011). URL: `http://bicycle.tudelft.nl/schwab/wb1413spring2013/MultibodyDynamicsB.pdf` (accessed May 8, 2014).
26. M. Haberland, "Extracting Principles from Biology for Application to Running Robots" *Ph.D. Thesis* (Massachusetts Institute of Technology, 2014).
27. T. McGeer, "Passive bipedal running," *Proc. R. Soc.* **240**(1297), 107–134 (1990).
28. D. G. E. Hobbelen and M. Wisse, "A disturbance rejection measure for limit cycle walkers: The gait sensitivity norm," *IEEE Trans. Robot.* **23**(6), 1213–1224 (2007).
29. S. M. Bruijn, O. G. Meijer, P. J. Beek and J. H. Van Dieën, "Assessing the stability of human locomotion: A review of current measures," *J. R. Soc. Interface* **10**(83) (2013).
30. D. L. Jindrich *et al.*, "Dynamic stabilization of rapid hexapedal locomotion," *J. Exp. Biol.* **205**(18), 2803–2823 (2002).
31. J. G. D. Karssen and M. Wisse, "Running with improved disturbance rejection by using non-linear leg springs," *Int. J. Robot. Res.* **30**(13), 1585–1595 (2011).
32. T. McGeer, "Passive dynamic walking," *Int. J. Robot. Res.* **9**(2), 62–82 (1990).
33. J. Pratt, C. M. Chew, A. Torres, P. Dilworth and G. Pratt, "Virtual model control: An intuitive approach for bipedal locomotion," *Int. J. Robot. Res.* **20**(2), 129 (2001).
34. M. Wisse, A. L. Schwab, R. Q. van der Linde and F. C. T. van der Helm, "How to keep from falling forward: Elementary swing leg action for passive dynamic walkers," *IEEE Trans. Robot.* **21**(3), 393–401 (2005).
35. B. S. Blanchard, D. Verma and E. L. Peterson, *Maintainability: A Key to Effective Serviceability and Maintenance Management*, vol. 13 (Wiley-Interscience, Hoboken, NJ, 1995).